Identification and characterisation of the CD40-ligand of *Sigmodon hispidus*

Marsha S. Russell[1], Abenaya Muralidharan[1,2], Louise Larocque[1], Jingxin Cao[3], Yvon Deschambault[3], Jessie Varga[3], Sathya N. Thulasi Raman[1], Xuguang Li[1,2]*

1 Centre for Biologics Evaluation, Biologics and Genetic Therapies Directorate, HPFB, Health Canada and WHO Collaborating Center for Standardization and Evaluation of Biologicals, Ottawa, Ontario, Canada, **2** Department of Biochemistry, Microbiology and Immunology, Faculty of Medicine, University of Ottawa, Ottawa, Canada, **3** National Microbiology Laboratory, Public Health Agency of Canada, Winnipeg, Manitoba, Canada

* sean.li@canada.ca

Abstract

Cotton rats are an important animal model to study infectious diseases. They have demonstrated higher susceptibility to a wider variety of human pathogens than other rodents and are also the animal model of choice for pre-clinical evaluations of some vaccine candidates. However, the genome of cotton rats remains to be fully sequenced, with much fewer genes cloned and characterised compared to other rodent species. Here we report the cloning and characterization of CD40 ligand, whose human and murine counterparts are known to be expressed on a range of cell types including activated T cells and B cells, dendritic cells, granulocytes, macrophages and platelets and exerts a broad array of immune responses. The cDNA for cotton rat CD40L we isolated is comprised of 1104 nucleotides with an open reading frame (ORF) of 783bp coding for a 260 amino acid protein. The recombinant cotton rat CD40L protein was recognized by an antibody against mouse CD40L. Moreover, it demonstrated functional activities on immature bone marrow dendritic cells by upregulating surface maturation markers (CD40, CD54, CD80, and CD86), and increasing IL-6 gene and protein expression. The availability of CD40L gene identity could greatly facilitate mechanistic research on pathogen-induced-immunopathogenesis and vaccine-elicited immune responses.

1. Introduction

The cotton rat (*Sigmodon hispidus*) was first used in polio research in the 1930s [1], and throughout the last century, it has proven to be an excellent model for biomedical research [2, 3, 4]. Historically in biomedical research, the mouse has been exploited as the default animal model. This is in part due to its well defined immunological and genetic information, cost-effectiveness, and abundant inbred strains and research reagents. However, the use of mice as models to study infectious diseases has its limitation since mice are not naturally infected by most human pathogens. On the other hand, cotton rat is susceptible to many human pathogens and is the ideal model of choice for measles (paramyxovirus) [5], herpes simplex (oral

and ophthalmic) [6], influenza (orthomyxovirus) [7, 8], HIV-1 [9], RSV (respiratory syncytial virus) [10], adenovirus [11, 12], human parainfluenza [13], and human metapneumovirus [14]. This model has been valuable for adenovirus-based gene replacement therapy research [15, 16], and was also proven to be indispensable in pre-clinical evaluation of the prophylactic antibodies (RespiGam® [17], and Synagis® [18]. Indeed, the cotton rat model was found to be valuable in terms of its biological and immunological relevance, it was deemed unnecessary to test the adenovirus-based gene therapy and the Synagis® prophylactic treatment against RSV disease in non-human primate prior to the human trials [19, 20].

A number of methods and reagents have been developed for the analysis of immune responses in cotton rats over the last decade. Up to date, more than 200 genes encoding cytokines, chemokines, cell surface markers and regulatory molecules have been cloned, with various related research reagents being commercially available. As a result, the use of cotton rats in pathogenesis studies addressing mechanistic questions has significantly increased. Nevertheless, the gene encoding CD154 and CD40 ligand (CD40L), remains elusive.

CD40L plays a critical role in orchestrating immune responses against pathogens. Depending on the post-translational modification, the murine CD40L is a 32–39 kDa type II membrane glycoprotein that was initially identified as a surface marker exclusive to activated CD4$^+$ T cells [21, 22]. It is a member of the TNF superfamily consisting of a sandwiched extracellular structure composed of a β-sheet, α-helix loop, and a β-sheet, allowing for the trimerization of CD40L, an additional feature of the TNF family of ligands [23]. Since its initial discovery, CD40L has been shown to be not only expressed on CD4+ T cells, but on dendritic cells (DCs) [24], B cells [25], and platelets [26].

It has been shown that upon interacting with its receptor, CD40, CD40L induces profound effects on T cells, DCs, B cells, endothelial cells, as well as many cells of the hematopoietic and non-hematopoietic systems. Moreover, when CD40L engages CD40 on the surface of DCs, it promotes cytokine production, the induction of cell surface co-stimulatory molecules, and facilitates the cross-presentation of antigen by these cells [27], enabling DCs to mature and effectively induce the activation and differentiation of T cells. When CD40L engages CD40 on the surface of B cells, it promotes germinal center formation, immunoglobulin (Ig) isotype switching, somatic hypermutation to enhance antigen affinity, and lastly, the formation of long-lived plasma cells and memory B cells [28].Various studies have been conducted to utilize gene delivery of CD40L to DCs and tumor cells for tumor immunotherapy. It was found that expression of CD40L in a small proportion of tumor cells was sufficient to generate a long-lasting systemic anti-tumor immune response in mice that was shown to be dependent on cytotoxic T lymphocytes [29, 30].

Here we report the successful cloning of the gene encoding cotton rat CD40L (crCD40L); we also expressed and purified the CD40L produced in mammalian cells. Further characterisation of the recombinant cotton rat CD40L revealed its functional activities in promoting DC maturation and cytokine production.

2. Materials and methods

2.1 Animals and ethics statement

6–7 weeks old cotton rats were obtained from an inbred colony maintained at Envigo (USA). All animal experiments were conducted in accordance with Institutional Care and Use Committee (IACUC) of Health Canada Ottawa Animal Care Committee which approved this study. The rats were housed 3 animals per cage in Allentown NexGen individually ventilated cages with free access to food and water. These cages provided a floor space of 142 in^2/ 916 cm^2. Body weight and any sign of distress were monitored daily. If anything associated the

animal health was observed, a full examination would be conducted. As In this study spleen cells from normal, healthy animals were isolated, we did not observe any adverse reaction. To isolate splenocytes from the animals, isoflourane was used to put the animals to sleep via inhalation with oxygen for euthanasia.

2.2 Isolation and sequence determination of cotton rat CD40L cDNA

The spleens from three naïve cotton rats were removed aseptically and snap frozen in liquid nitrogen. The spleens were homogenized individually with a TissueLyser II (Qiagen) and total RNA extracted using the RNeasy Mini kit (Qiagen) with on-column DNase digestion according to the user's manual. The 3' RACE system (Life Technologies) was then used with to amplify the 3' portion of the cotton rat CD40L from the total RNA according to the manufacturer's instructions. A schematic of the 3' RACE procedure used is provided in S1 Fig. A gene specific primer (5'–GGACTCTATTATGTCTACACCCAAGTCACCTTCTG -3') was derived from a consensus sequence aligning the rat (*Rattus norvegicus* UniProt: Q9Z2V2), mouse (*Mus musculus* UniProt: P27548), and golden hamster (*Mesocricetus auratus* NCBI Reference Sequence: XM_005084522.3) CD40L sequences obtained from the National Center for Biotechnology Information (NCBI). Following first strand cDNA synthesis, the 3' portion of the cotton rat CD40L mRNA was PCR amplified using the consensus sequence derived gene specific primer and the abridged universal amplification primer with an annealing temperature at 56˚C. The reverse complementary sequence of this primer was then used as a reverse primer with the forward primer (5'—GATAGAAACATACAGCCAACCTTCTCCCAGATC -3') to amplify the 5' portion of the cotton rat CD40L mRNA with an annealing temperature of 57˚C.

All amplified fragments were sequenced with BigDye Terminator v.3.1 Cycle Sequencing kit (ThermoFisher cat # 4336917). Briefly, samples were amplified in a PTC-200 thermal cycle (MJ Research) with the following program: 26 cycles of 1˚C/S to 96˚C, 96˚C for 10 seconds, 1˚C/S to 50˚C, 50˚C for 5 seconds, 1˚C/S to 60˚C, 60˚C for 4 minutes. The samples were cleaned using DyeEx 2.0 Spin kit (Qiagen cat # 63204) and loaded onto a 3130xl Genetic Analyzer (Applied Biosystems). Raw sequencing data was edited by the instrument's software (ThermoFisher 3130xl Genetic Analyzer Data Collection Software v3.0), and then imported into GeneCodes Sequencher v4.6.1 sequencing analysis software for further editing. The final sequenced contigs are then imported to NCBI BLAST (https://blast.ncbi.nlm.nih.gov/Blast.cgi) to confirm the identity.

2.3 Sequence and phylogenetic analysis

Putative conserved domains, trimer interface, and receptor binding sites were determined by performing a standard protein BLAST (blastp algorithm; https://blast.ncbi.nlm.nih.gov). The sequences producing significant alignments were imported into Geneosis software, (Auckland, New Zealand). Multiple alignment was conducted as previously described [31], with phylogenetic analysis using Geneosis Pro 5.6.7.

2.4 Cloning of crCD40L into vaccina virus expression system

Once the mRNA sequence was confirmed, a construct was designed beginning with a kozak sequence (5'– CACCGCCGCCACC– 3'), followed by a secretion signal consisting of 23 amino acid (aa) (MLLAVLYCLLWSFQTSAGHFPRA) from the human tyrosinase signal peptide as previously described [32]. This is followed by six histidine residues to facilitate protein purification. Following this sequence, a 27-aa fragment from the bacteriophage T4 fibritin trimerization motif was added [33] and finally connected to the full length 783bp open reading frame

(ORF) of the cotton rat CD40L sequence at the C terminus. This construct was synthesized and cloned into pUC57 (Biobasic, Markham, ON).

Generation of a recombinant vaccinia virus expressing cotton rat CD40L protein construct was achieved using a vaccinia virus E3L and K3L double deletion mutant virus as the parental virus and taterapoxvirus K3L as the positive selection marker (Jingxin Cao, unpublished information). Briefly, the recombination plasmid vector for expression of the CD40L construct gene consists of the homologous flanking vaccinia DNA sequences targeting vaccinia A45R gene (SOD homolog); the CD40L construct gene driven by a modified vaccinia H5 promoter (Vaccine 1996, 14:1451), and taterapoxvirus 037 gene driven by vaccinia K3L promoter as the positive selection marker. The recombination vector was transfected into a HeLa PKR knockout cells infected with a vaccinia virus with both E3L and K3L genes deleted. Selection and purification of the recombinant vaccinia virus expressing the CD40L was done in BHK21 cells.

2.5 Western blot

Expression of the CD40L protein was confirmed by Western blotting using His-tag Ab. Cell monolayers were lysed in sample buffer and homogenized using QIAshredder columns (Qiagen). Western blotting was performed using 4 to 15% TGX gel and Tris/Glycine/SDS running buffer (Bio-Rad Laboratories Inc.), and the protein samples were transferred to Immobilon-FL PVDF membranes (Millipore). Protein was detected with Tetra-HIS Ab (Qiagen) and goat anti-mouse IRDye-800CW (LiCor). Membranes were developed using the Odyssey system (LiCor).

2.6 Expression and purification of recombinant crCD40L

The vaccinia virus carrying the crCD40L gene was propagated in BHK21 cells. The cells were collected and washed with PBS once and then lysed with a denaturing buffer (10 mM Tris–HCl, 100 mM sodium phosphate, 6 M guanidine hydrochloride, 10 mM reduced glutathione, pH 8.0) and disrupted by sonication on ice using a Branson sonifier 150 (ThermoFisher, Waltham, MA) at level 1 for two 10sec bursts with 1min rest on ice between. After separation of cell debris, the supernatant was added to a slurry of Ni-NTA resin (Qiagen, Mississauga, ON, Canada) (10 mL resin bed) and stirred at room temperature for 30 min before loading into a column. The column was purified using an AKTA purifier (Amersham Biosciences) with Unicorn 5.3 software (Amersham Biosciences). Refolding was accomplished under oxidative conditions with a gradient of denaturing buffer to buffer B (buffer B: 10 mM Tris–HCl, 100 mM sodium phosphate, pH 7.8) over 10 column volumes (CVs). The column was then washed with three CVs of buffer B + 60 mM imidazole (pH 7.8) to remove unspecific binding. The protein was eluted off the column with buffer B + 250 mM imidazole (pH 7.8). The resulting protein was dialysed against PBS pH 7.5 and then confirmed by western blot.

2.7 Enzyme-linked immunosorbant assay (ELISA)

96-well plates were coated with either recombinant mouse CD40L (R&D Systems) or the recombinant crCD40L protein 2ug/ml in 100μl PBS. Plates were washed with wash buffer (PBS-0.1% tween-20) and then blocked with 200μl/well blocking buffer (PBS containing 0.1% Tween 20 and 3%IgG Free BSA) for 1 hour at 37˚C. Plates were washed with wash buffer and incubated at 37˚C for 1 hour with 100μl/well goat anti-mouseCD40L (R&D Systems) 2ug/ml in blocking buffer. Plates were subsequently washed and incubated at 37˚C for 1 hour with 100μl/well with rabbit anti-goat IgG HRP conjugate (Zymed). Plates were washed again and incubated for 10 min in the dark with 100μl/well 3,3'5,5'-tetramethylbenzidine substrate (New

England Bio Labs). The reaction was stopped with Stop solution (New England Bio Labs) and absorbance was read at 450nm on a BioTek Synergy 2 plate reader.

2.8 Maturation and activation analysis of mouse bone marrow DC

Primary bone marrow cells from Balb/c mice (Chicago, IL) were thawed and cultured in dendritic cell medium from manufacture (Cell Biologics M7711) supplemented with GMCSF (Cell Biologics) without IL-4 at $4x10^5$ cells/well in a volume of 200μl. The cells were treated with 0.5μg/ml recombinant mouse CD40L (Preprotech, Montreal, QC) or the recombinant crCD40L protein at 0.5μg/ml, 5μg/ml, or 50μg/ml. Forty hours later, flow cytometry was performed on a BD LSRFortessa cell analyser after 2×10^5 cells/tube were stained using CD11c-PE-CF594, CD54-FITC, CD40-BV786, CD80-BV421, and CD86-BV711 antibodies. All antibodies were purchased from BD Biosciences. The resulting spectra were analysed using FACS-Diva version 8.0.1 software.

To assess IL-6 mRNA production of immature bone marrow murine DCs in response to targeting by recombinant crCD40L, quantitative real-time PCR was conducted on an ABI Prism 7500 Fast Sequence detection system (Applied Biosystems). TaqMan assay reagent kits (Applied Biosystems) were used that contain pre-standardized primers and TaqMan MGB probes for IL-6 and 18S which were used to normalize the data. Total RNA was isolated from $8x10^5$ stimulated bone marrow DCs using the RNeasy Mini Kit (Qiagen) according to manufactures instructions. The isolated RNA was used to make cDNA using the Superscript III First-Strand Synthesis System for RT-PCR (Invitrogen) according to manufacturer's instructions. The cDNA was then subjected to quantitative PCR using the TaqMan Fast Advanced Master Mix (Applied Biosystems) according to manufactures instructions. Samples were run in duplicate and C_t values were obtained. Fold change over unstimulated DCs was calculated using the $2^{-\Delta\Delta CT}$ method of relative quantification [34], using 18S as the housekeeping reference gene. To investigate IL-6 secretion by murine bone marrow DCs, supernatant from forty hour stimulated cultures were collected and assayed using the Mouse IL-6 DuoSet ELISA Kit (R & D Systems) following the manufacturer's protocol.

3. Results and discussion

3.1 Sequence determination of the cotton rat CD40L coding sequence

The complete mRNA sequence of CD40L was obtained in two steps (Fig 1). A sequence corresponding to nucleotides 535 through to the poly-A tail was obtained using the 3' RACE kit and mRNA as starting material, which was isolated from cotton rat splenocytes and a rodent consensus sequence as a primer. This portion of the sequence has the 3' un-translated region of the mRNA as well as the stop codon. The 5' end of the protein was obtained in the next step by PCR amplification of the cDNA obtained in the first step with the 3' RACE kit and the reverse complement of the consensus sequence primer and a second consensus sequence primer designed to bind to the beginning of the CD40L mRNA. The 783bp ORF encodes 260aa followed by a stop codon.

Comparison of the sequenced CD40L gene revealed that the crCD40L coding sequence shares 93%, 89%, and 83%, identity with golden hamster, rat, and mouse, respectively. At the amino acid (aa) level, the corresponding identities are 91%, 82%, and 82%, Fig 2a. At both the mRNA and aa levels, the crCD40L shared the closest similarity with Peromyscus maniculatus bairdii (or deer mouse) at 93% and 92% respectively. When sequence homology analysis is performed, crCD40L clusters with other members of the Cricetidae family Fig 2b.

We next examined the functional domains in crCD40L in comparison with other known CD40L. As shown in Fig 3a, crCD40L has a putative tumor necrosis factor (TNF) superfamily

5'-
ATGATAGAAACATACAGCCAACCTTCTCCCCGATCCGTGGCTACTGGGCTGCCCGTCAGCATGAAAATTTTTATGTATTT
ACTTACTGTTCTTCTCATCACCCAGATGATTGGGTCAGTGCTTTATGCTGTGTATCTTCATAGAAGACTGGACAAGGTAG
AAGAGGAAGTAAGCCTTCATGAAGATTTTGTATTCATAAAAAAGCTACAGAGATGCATCAAAGGAGAAGGATCCTCAT
CCTTGCTGAACTGTGAGGAGGTGAGAAGGCGATATGAAGACCCTGTCAAGGATATAAGGTTAAACAAAGAAGATAAA
AAAGAAATCAGCTATGAAATGCAAAAAGGTGATGAGGAGCCTCAAATTGCAGTACATGTTGTAAGTGAGGCCAACAG
CAAAACAACATCTGTTCTACAGTGGGCCAAGAAAGGATATTATACCATGAAAAACAACTTGGTAATGCTCGAAAGTGGT
AAACAGCTGACTATTAAAAGACAAGGACTCTATTATATCTACACCCAAGTCACCTTCTGTTCTAATCAGGAACCTACGAG
TAAAGATCCATTTTTAGTCAGCCTCTGTCTGAAGTCCACCAGTGGATCTGAGAGAATCTTGCTCAGGGCAGCAAACAC
CCACAGTTCCTCCAAGCCCTGTGGCCAACAGTCGGTTCATTTGGGAGGAGTATTTGAATTACAAGAAGATTCTTCTTTG
TTCGTCAACGTGACTGATGCAAGCCAAGTGATCCATGGAATCGGCTTTACATCTTTTGGCTTACTCAAACTCTGAACAG
TGTGCTGTCCTAGGCTGCAGCAGGGCTGATGCTGGCAGTCTTCCCAAAACAGCAAATCAGTTAGGACCCGCCCCCTGT
TGAACTGCCTATTTATAACCCTTGGACCCTCCTCACAGAGAACTATTTATTATATACCCCAAGGAAATAAGAAATAAGAG
AATTACAGGGCAGGCAAAAATCCTAATGGACCCTGCTCCATAAGAGCTTATCATCTTAAATAGCAACTCTACTGATGCAT
ACAACCAGAGAGCCCTAGGAAAAGACAAAGCCATAATGTACAGATGACAGAGCTCCAATGAAACAGCAGATAATTGA
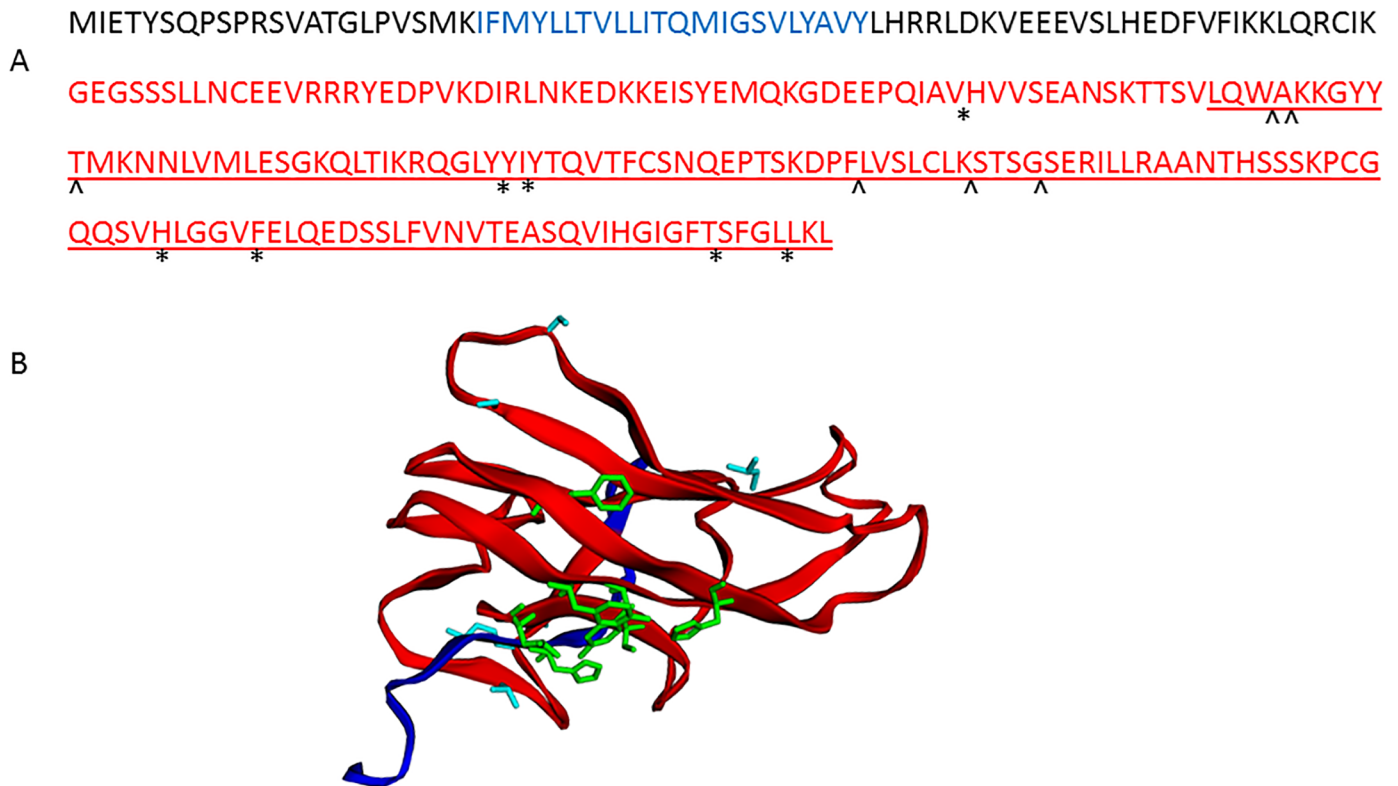CCAAAAAAAAAAAAAAAAAAAA – 3'

Fig 1. Cotton rat CD40L mRNA sequence. The sequence was determined using 3' RACE of mRNA extracted from the spleen of a cotton rat.
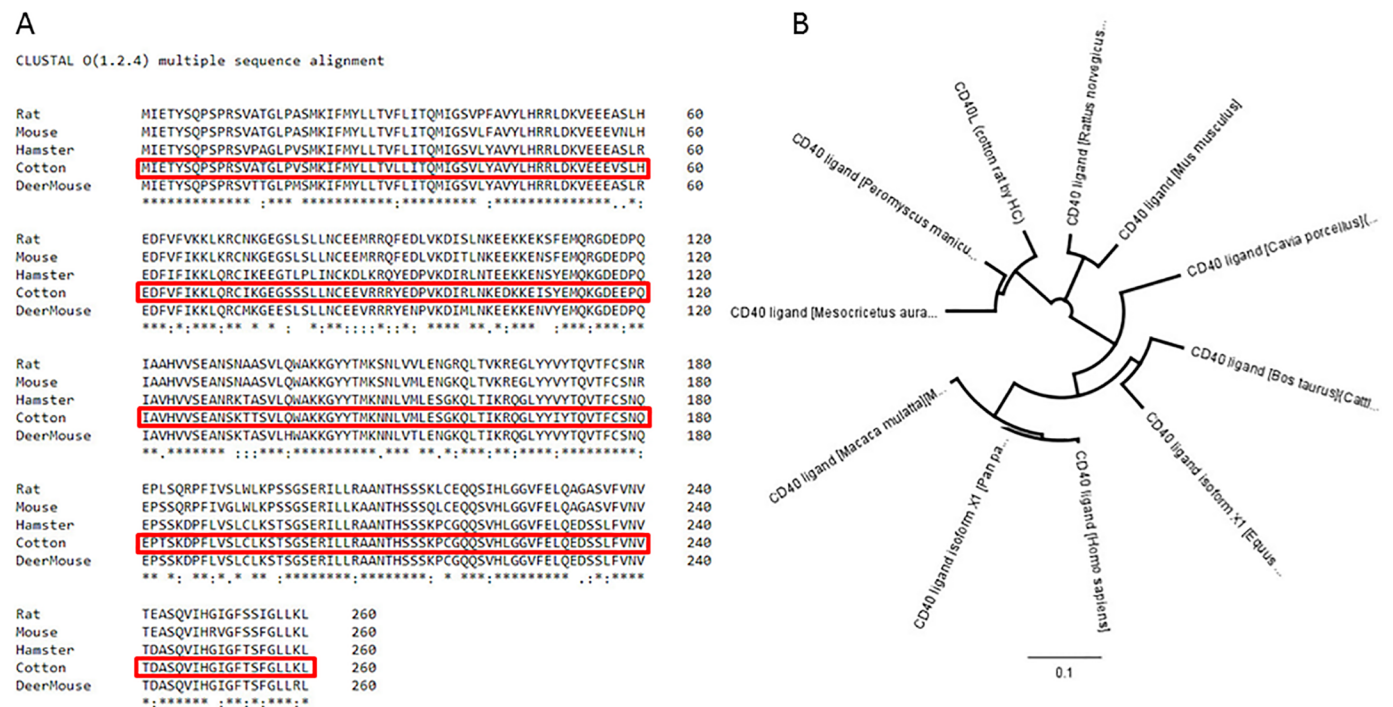
Fig 2. Sequence alignment of cotton rat CD40L. (A) The Clustal Omega sequence alignment program from EMBL-EBI was used to align the protein sequence of crCD40L with those of other closely related species. Rat (*Rattus norvegicus* UniProt: Q9Z2V2), Mouse (*Mus musculus* UniProt: P27548), Golden Hamster (*Mesocricetus auratus* NCBI Reference Sequence: XM_005084522.3), and Deer Mouse *Peromyscus maniculatus bairdii* (NCBI Reference Sequence: XP_006992033). An * (asterisk) indicates positions which have a single, fully conserved residue. A: (colon) indicates conservation between groups of strongly similar properties—scoring > 0.5 in the Gonnet PAM 250 matrix. A. (period) indicates conservation between groups of weakly similar properties—scoring = < 0.5 in the Gonnet PAM 250 matrix. (B) Alignment tree was produced using Geneosis software and multiple alignment was conducted with phylogenetic analysis.

A

MIETYSQPSPRSVATGLPVSMKIFMYLLTVLLITQMIGSVLYAVYLHRRLDKVEEEVSLHEDFVFIKKLQRCIK

GEGSSSLLNCEEVRRRYEDPVKDIRLNKEDKKEISYEMQKGDEEPQIAVHVVSEANSKTTSVLQWAKKGYY
                                                          *   ^^

TMKNNLVMLESGKQLTIKRQGLYYIYTQVTFCSNQEPTSKDPFLVSLCLKSTSGSERILLRAANTHSSSKPCG
^   * *   ^   ^   ^

QQSVHLGGVFELQEDSSLFVNVTEASQVIHGIGFTSFGLLKL
    *   *   *   *

B

Fig 3. Cotton rat CD40L putative conserved domains. (A) (-) A line below the sequence indicates the putative TNF superfamily domain. (*) Putative trimer interface on conserved domain TNF. (^) Putative receptor binding sites on conserved domain TNF. The putative transmembrane domain is shown in blue. The putative ecto domain from aa 115 through to aa 260 is shown in red. (B) Image of monomer of Cotton Rat CD40L putative ectodomain conserved regions. The putative TNF superfamily domain is shown in red. (*) Putative trimer interface on conserved TNF superfamily domain residues are shown in green. (^) Putative receptor binding sites on conserved TNF superfamily domain are shown in light blue.

https://doi.org/10.1371/journal.pone.0199067.g003

domain (aa 137–260) and a 23 aa putative transmembrane domain (aa 23–45). Amino acids 124, 169, 171, 223, 228, 254, and 258 comprise the putative trimer interface, while amino acids 140, 141, 146, 189, 196, and 200 comprise the putative receptor binding sites.

Using EZmol software [35], we predicted folding of the protein as shown in Fig 3b. The cotton rat CD40L cDNA that we have isolated was a 1104 nucleotide sequence with a poly-A tail containing an ORF of 783bp which coded for a 260 aa protein. The homology of cotton rat CD40L, at both the amino acid and nucleic acid level, is closer to members of the Cricetidae family (hamster and deer mouse) than to those of the Muridae family (rat and mouse) as shown in Fig 2b. As with other known CD40L proteins, there is a putative TNF superfamily domain, a transmembrane domain, trimerization sites, and receptor binding sites [36].

TNF superfamily members include TNF (TNF-alpha), LT (lymphotoxin-alpha, TNF-beta), CD40 ligand, Apo2L (TRAIL), Fas ligand, and osteoprotegerin (OPG) ligand, among others [37]. The TNF superfamily is composed of 19 ligands and 29 receptors, in which each has vastly diversified roles in the body and exhibit pro-inflammatory activity, partly via activation of NF-kB [37]. Members of this family generally have an intracellular N-terminal domain, a short transmembrane segment, an extracellular stalk, and a globular TNF-like extracellular domain of about 150 residues [23]. They initiate apoptosis by binding to related receptors, some of which have intracellular death domains [38]. These proteins typically form homo- or hetero- trimeric complexes and bind one elongated receptor molecule along each of three

clefts formed by neighboring monomers of the trimer and ligand trimerization is for receptor binding [23, 39]. All seven known conserved residues that constitute the trimer interface on the conserved TNF domain [23, 40], were mapped to the putative crCD40L protein sequence. Additionally, all six known conserved receptor binding sites on the conserved TNF domain [23, 40], were mapped to the crCD40L protein sequence.

3.2 Expression of recombinant cotton rat CD40L in vaccinia virus

In order to further evaluate the crCD40L deduced sequence, the full 783bp ORF of the crCD40L was cloned into a vaccinia virus vector. The crCD40L construct was designed to carry a secretion signal, histidine tag, and a trimerization motif (Fig 4a). Selection and purification of the recombinant vaccinia virus expressing the CD40L construct was conducted in BHK21 cells. Western blot with anti-histidine antibody (Ab) was used to confirm expression of the CD40L protein construct Fig 4b and S2 Fig. The resulting 36 kDa protein product was found in both the cell lysate and supernatant (faint band—48 hours only). Since the highest expression was found in the cell lysate, it was used for further purification of the protein. It should be noted that the protein was only able to be detected under reducing conditions. Under non-reducing conditions, the protein was unable to be detected by the anti-histidine Ab, even in the cell lysate (data not shown). This indicates that the histidine tag is folded within the trimer and is unavailable in the native form for purification. This is an additional reason for the need to purify the protein from the cell lysate under harsh denaturing conditions followed by protein refolding. The reason we utilized a mammalian expression system to produce the protein rather than a bacterial system is to facilitate its proper folding into its native structure, trimerization, and glycosylation. The aa backbone predicts a protein of 29 kDa, yet initial studies of the CD40L protein suggested a molecular mass of 39 kDa, and on most cell types the
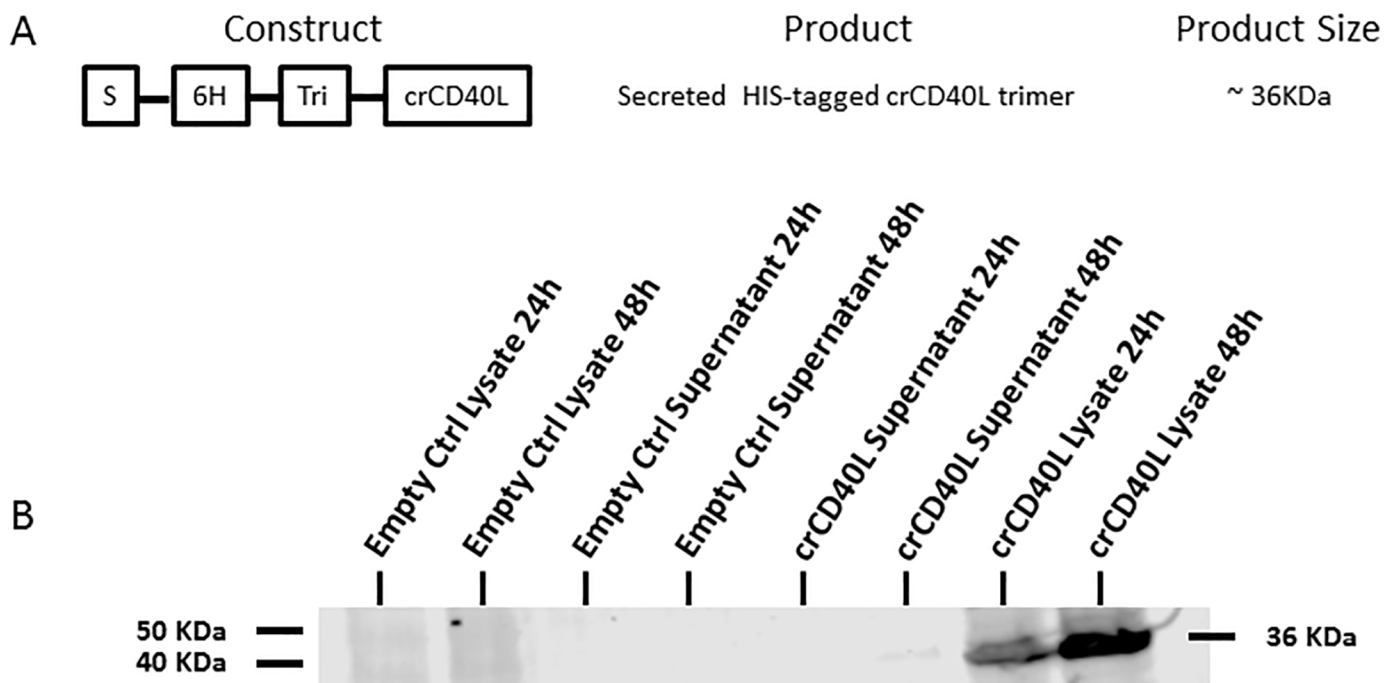
Fig 4. crCD40L construct and protein expression and secretion. (A) Schematic representation of the vv-crCD40L construct. Where "S" is the secretion signal, "6H" is a six histidine residue, and "Tri" is the trimerization motif. (B) In vitro protein expression in BHK21 cell lysate and supernatant collected 24h and 48h post infection. Protein expression is confirmed by Western blot using an anti-histidine Ab.

molecular mass of CD40L is 32-33kDa, consistent with extensive post-translation modification [36].

3.3 Purification and verification of cotton rat CD40L

The BHK21 cells expressing the crCD40L construct were collected and lysed with 6 M guanidine hydrochloride with reduced glutathione and sonication. The lysate was loaded on the nickel column and the washed with denaturing buffer as described in materials and methods. The bound proteins were refolded on the column with gradient buffer exchange, to allow slow refold the protein, given that CD40L biological activity is dependent on a homo-trimer configuration [23]. The resulting bound protein was subsequently eluted with imidazole. The resulting fractions that showed a peak were pooled and dialysed against PBS.

The purified protein was confirmed in ELISA. Since the cotton rat CD40L protein sequence shared 82% identity with the mouse CD40L protein sequence, an Ab known to detect mouse CD40L was used to identify the purified crCD40L protein. The purified recombinant crCD40L was used as a coating antigen in a concentration gradient manner, and was detected with an Ab generated against the mouse CD40L at all concentrations (Fig 5). Uncoated controls were performed in parallel and were negative for CD40L in ELISA. We measured the overall strength of the antigen-antibody complex in the presence of 6M urea [41]. The avidity of the cotton rat CD40L for the anti-mouse CD40L antibody was decreased in the presence of 6M urea at all concentrations. Clearly, as the antibody used was raised against mouse CD40L, the
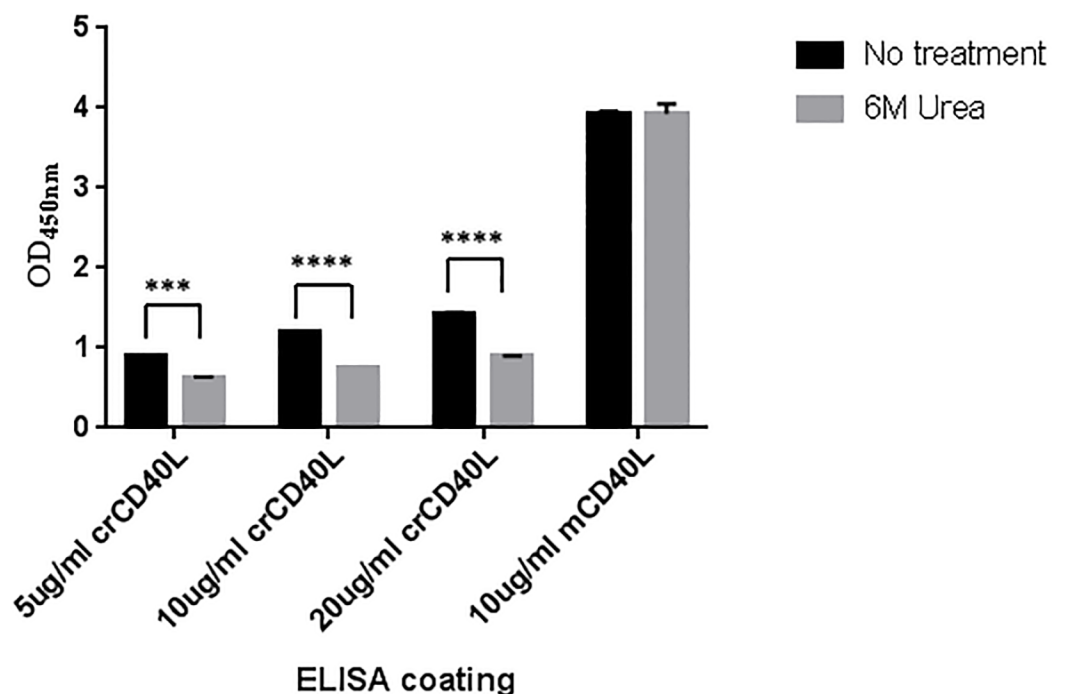
Fig 5. crCD40L is detected by mouse CD40L. crCD40L was expressed in vaccinia virus and purified from infected BHK21 cell lysate on a nickel column. The purified protein was detected by ELISA using a mouse antibody against CD40L in a concentration gradient dependent manner. The avidity of the mouse CD40L antibody to the cotton rat CD40L protein was evaluated in the presence of 6M urea. The difference between the untreated and 6M urea treated for each group was calculated using students t-test ***$p<0.001$, ****$p<0.0001$ (n = 2). Data shown is a representative experiment of three separate experiments where two (n = 2) technical replicates are conducted in each experiment. The no-coating and no-primary antibody negative controls gave average OD values of 0.56 and 0.107 respectively.

https://doi.org/10.1371/journal.pone.0199067.g005

Table 1. crCD40L upregulates expression of mouse DC maturation markers as measured by MFI.

	U/T		mCD40L 3ug/ml		crCD40L 3ug/ml		crCD40L 30ug/ml	
Marker	MFI	95%CI	MFI	95%CI	MFI	95%CI	MFI	95%CI
CD11c	12,131	11752 to 12131	9,921	9921 to 10251	11,515	11515 to 11966	8,960	8960 to 10472
CD54	2,742	2713 to 2770	2,944	2758 to 2944	3,052	2750 to 3052	2,997	2795 to 2997
CD40	347	330 to 383	794	726 to 794	296	259 to 296	544	497 to 544
CD80	754	731 to 754	1,021	1021 to 1065	743	731 to 743	939	939 to 975
CD86	308	308 to 362	1,409	1409 to 1558	260	260 to 304	748	713 to 791
I-A^d	2,516	2424 to 2596	3,797	3613 to 3797	2,255	2255 to 2425	2,970	2295 to 2974

U/T: Unstimulated; MFI: Median Fluorescence Intensity; CI: 95% confidence Interval; MFI data are a representative of three separate experiments

addition of urea treatment would substantially weaken the interaction between the antibody and crCD40L.

3.4 Functional activity of the recombinant crCD40L

Since the cotton rat CD40L protein sequence shared 82% identity with the mouse CD40L protein sequence with similar functional domains, we evaluated the biological activity of the recombinant crCD40L on immature murine bone marrow DCs. We conducted experiments based on known functional activities of CD40L in other animal species. Specifically, maturation of immature DCs after exposure to antigen is known to play a crucial role in their immunity-stimulating function [36], while trimeric recombinant CD40L has been shown to stimulate DC immunomodulating functions [42]. When CD40L engages CD40 on the surface of DCs, it promotes cytokine production, the induction of cell surface co-stimulatory molecules, and facilitates the cross-presentation of antigen by these cells [27]. In addition, CD11c is a DC integrin marker and upon stimulation, is down-regulated [43]. Intracellular adhesion marker CD54, along with co-stimulatory markers CD40, CD80, and CD86 are all upregulated upon stimulation with CD40L [44, 45]. Moreover, mouse I-A^d major histocompatibility complex is also up-regulated upon stimulation with CD40L [45]. When our recombinant crCD40L was used to stimulate immature murine bone marrow DCs, we observed similar results to that when murine CD40L is used (Tables 1 and 2). CD11c was down regulated in both median flouresence intensity (Table 1) and the percentage of positive cells (Table 2). The co-stimulatory molecules CD54, CD40, CD80, and CD86 were all up-regulated in both median fluorescence intensity (Table 1) and the percentage of positive cells (Table 2). The Mouse I-A^d major histocompatibility complex was upregulated in median fluorescence intensity (Table 1) but

Table 2. crCD40L increases the percentage of cells expressing mouse DC maturation markers.

	U/T		mCD40L 3ug/ml		crCD40L 3ug/ml		crCD40L 30ug/ml	
Marker	%Positive cells	95% CI	%Positive cells	95% CI	%Positive cells	95% CI	%Positive cells	95% CI
CD11c	28	27 to 29	13	12 to 13	23	23 to 28	9	8 to 9
CD54	0	0 to 1	4	3 to 4	0	0 to 1	2	2 to 3
CD40	57	53 to 66	78	76 to 81	52	52 to 62	69	64 to 73
CD80	59	56 to 60	71	71 to 76	58	57 to 58	71	71 to 76
CD86	36	36 to 38	68	62 to 69	34	34 to 37	66	56 to 66
I-A^d	94	93 to 94	95	95 to 95	93	90 to 93	93	93 to 94

U/T: Unstimulated; CI: 95% Confidence Interval; data are a representative of three separate experiments

not up-regulated in terms of the overall percentage of positive cells (Table 2). We speculate this to be due to the species incompatibility since we are stimulating mouse bone marrow cells with cotton rat CD40L. Nevertheless, the crCD40L was able to promote up-regulation of key co-stimulatory markers on immature DCs promoting DC maturation. The gating strategy used for the flow cytometry analysis is provided in S3 Fig along with overlapping histograms of the intracellular adhesion marker and co-stimulatory markers.

CD40-induced activation of cytokine gene expression in DCs by CD40L is an important process in the initiation of primary immune responses and is critical for DC maturation and the generation of antigen-specific T cell responses [46]. IL-6 is a highly pleiotropic cytokine in that it stimulates the activation, proliferation, and survival of T cells, and furthermore, modifies DC function and survival [47–50]. We tested if the recombinant crCD40L could induce IL-6 gene expression (Fig 6a) and production of the cytokine (Fig 6b) by immature murine bone marrow DCs. The results indicate that a significant increase in both IL-6 gene expression and cytokine production in immature murine bone marrow DCs was observed forty hours after stimulation with the crCD40L. Collectively, the observation that both the upregulation of immature DC cell surface maturation markers and increased IL-6 gene expression and cytokine production provide strong evidence of the biological activity of crCD40L.

In summary, the cotton rat CD40L cDNA that we isolated was a 1104 nucleotide sequence with a poly-A tail containing an ORF of 783 bp which coded for a 260 aa protein. The recombinant cotton rat CD40L was recognized by an Ab against mouse CD40L in direct ELISA, and showed biological activity by upregulating maturation markers (CD40, CD54, CD80, and CD86) as well as I-A^d on immature bone marrow murine DCs and moreover, inducing upregulation of IL-6 gene and cytokine expression in these cells.

The isolation of the cotton rat CD40L sequence and availability of CD40L has the potential to positively impact basic immunological research and vaccine development, given the critical importance of this protein in orchestrating immune responses [51, 52].
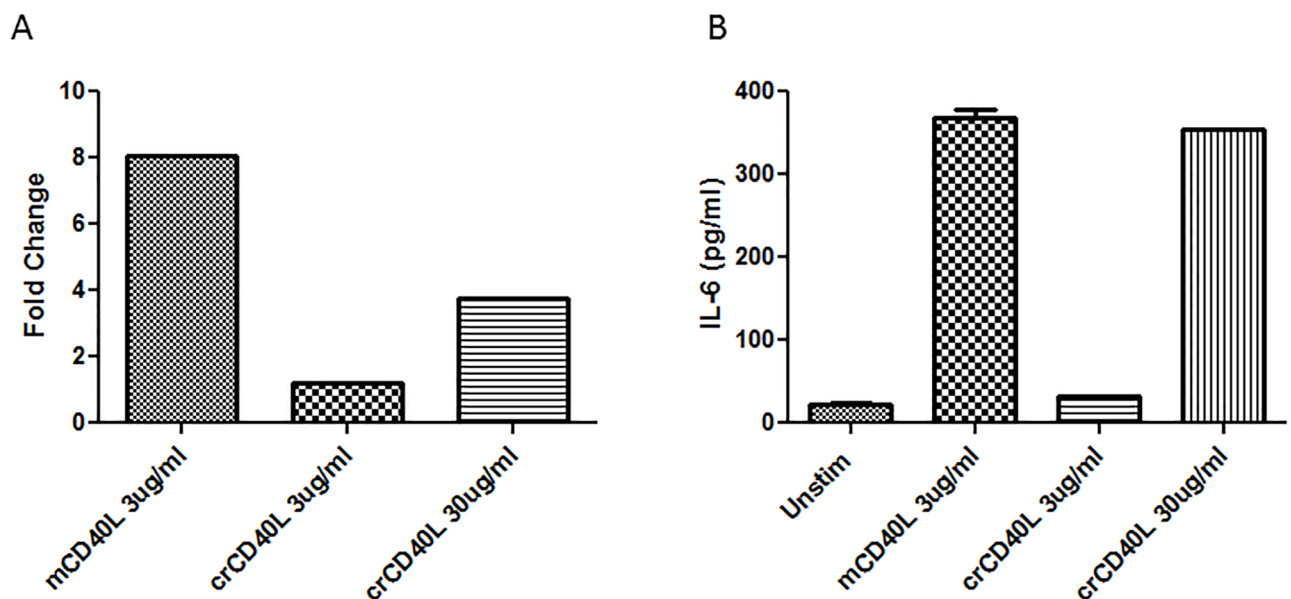
Fig 6. crCD40L induces IL-6 production in immature mouse dendritic cells. Immature mouse dendritic cells were stimulated with either recombinant mouse CD40L, or purified recombinant crCD40L for forty hours. (A) IL-6 gene expression was evaluated using quantitative real-time PCR using 18S to normalize the data. Data are presented as normalized fold change values over unstimulated DCs. These data are a representative of three separate experiments with two technical replicates per experiment. (B) IL-6 cytokine levels in the corresponding supernatant were evaluated using ELISA (n = 2). These data are a representative of three separate experiments with two technical replicates per experiment.

Supporting information

S1 Fig. Summary of the 3'RACE strategy used to elucidate the cotton rat CD40L gene sequence.
(PDF)

S2 Fig. crCD40L construct and protein expression and secretion.
(PDF)

S3 Fig. Gating strategy for flow cytometry analysis of dendritic cells.
(PDF)

Acknowledgments

Author Contributions

References

1. Armstrong C. The Experimental Transmission of Poliomyelitis to the Eastern Cotton Rat, Sigmodon hispidus hispidus. Public Health Reports. 1939; 54(38): p. 1719–1721

2. Faith R, Montgomery C, Durfee W, Aguilar-Cordova E, Wyde P. The cotton rat in biomedical research. Lab Anim. Sci. 1997; 47: p. 337–345 PMID: 9306305

3. Niewiesk S, Prince G. Diversifying animal models: the use of hispid cotton rats (Sigmodon hispidus) in infectious diseases. Lab Anim. 2002; 36(4): p. 357–372 https://doi.org/10.1258/002367702320389026 PMID: 12396279

4. Green M, Huey D, Niewiesk S. The cotton rat (Sigmodon hispidus) as an animal model for respiratory tract infections with human pathogens. Lab Anim (NY). 2013; 42(5): p. 170–176.

5. Wyde PR, Stittelaar KJ, Osterhaus AD, Guzman E, Gilbert BE. Use of cotton rats for preclinical evaluation of measles vaccines. Vaccine. 2000; 19(1): p. 42–53. PMID: 10924785

6. Boukhvalova M, McKay J, Mbaye A, Sanford-Crane H, Blanco JC, Huber A, et al. Efficacy of the Herpes Simplex Virus 2 (HSV-2) Glycoprotein D/AS04 Vaccine against Genital HSV-2 and HSV-1 Infection and Disease in the Cotton Rat Sigmodon hispidus Model. J Virol. 2015; 89(19): p. 9825–9840. https://doi.org/10.1128/JVI.01387-15 PMID: 26178984

7. Ottolini MG, Blanco JC, Eichelberger MC, Porter DD, Pletneva L, Richardson JY, et al. The cotton rat provides a useful small-animal model for the study of influenza virus pathogenesis. J Gen Virol. 2005; 86(10): p. 2823–2830.

8. Eichelberger MC. The cotton rat as a model to study influenza pathogenesis and immunity. Viral Immunol. 2007; 20(2): p. 243–249. https://doi.org/10.1089/vim.2007.0017 PMID: 17603841

9. Langley RJ, Prince GA, Ginsberg HS. HIV type-1 infection of the cotton rat (Sigmodon fulviventer and S. hispidus). Proc Natl Acad Sci U S A. 1998; 95(24): p. 14355–14360. PMID: 9826704

10. Boukhvalova MS, Blanco JC. The cotton rat Sigmodon hispidus model of respiratory syncytial virus infection. Curr Top Microbiol Immunol. 2013; 372: p. 347–358. https://doi.org/10.1007/978-3-642-38919-1_17 PMID: 24362698

11. Prince GA, Porter DD, Jenson AB, Horswood RL, Chanock RM, Ginsberg HS. Pathogenesis of adenovirus type 5 pneumonia in cotton rats (Sigmodon hispidus). J Virol. 1993; 67(1): p. 101–111. PMID: 8380066

12. Tsai JC, Garlinghouse G, McDonnell PJ, Trousdale MD. An experimental animal model of adenovirus-induced ocular disease. The cotton rat. Arch Ophthalmol. 1992; 110(8): p. 1167–1170. PMID: 1323254

13. Porter DD, Prince GA, Hemming VG, Porter HG. Pathogenesis of human parainfluenza virus 3 infection in two species of cotton rats: Sigmodon hispidus develops bronchiolitis, while Sigmodon fulviventer develops interstitial pneumonia. J. Virol. 1991; 65: p. 103–111. PMID: 1845878

14. Williams JV, Tollefson SJ, Johnson JE, Crowe JEJ. The cotton rat (Sigmodon hispidus) is a permissive small animal model of human metapneumovirus infection, pathogenesis, and protective immunity. J. Virol. 2005; 79: p. 10944–10951. https://doi.org/10.1128/JVI.79.17.10944-10951.2005 PMID: 16103146

15. Rosenfeld MA, Siegfried W, Yoshimura K, Yoneyama K, Fukayama M, Stier LE, et al. Adenovirus-mediated transfer of a recombinant alpha 1-antitrypsin gene to the lung epithelium in vivo. Science. 1991; 252(5004): p. 431–434. PMID: 2017680

16. Rosenfeld MA, Yoshimura K, Trapnell BC, Yoneyama K, Rosenthal ER, Dalemans W, et al. In vivo transfer of the human cystic fibrosis transmembrane conductance regulator gene to the airway epithelium. Cell. 1992; 68(1): p. 143–155. PMID: 1370653

17. Ottolini MG, Porter DD, Hemming VG, Zimmerman MN, Schwab NM, Prince GA. Effectiveness of RSVIG prophylaxis and therapy of respiratory syncytial virus in an immunosuppressed animal model. Bone Marrow Transplant. 1999; 24: p. 41–45. https://doi.org/10.1038/sj.bmt.1701813 PMID: 10435733

18. Ottolini MG, Curtis SR, Mathews A, Ottolini SR, Prince GA. Palivizumab is highly effective in suppressing respiratory syncytial virus in an immunosuppressed animal model. Bone Marrow Transplantation. 2002; 29: p. 117–120. https://doi.org/10.1038/sj.bmt.1703326 PMID: 11850705

19. Crystal RG. Adenovirus: The First Effective In Vivo Gene Delivery Vector. Hum Gene Ther. 2014; 25(1): p. 3–11. https://doi.org/10.1089/hum.2013.2527 PMID: 24444179

20. Sáez-Llorens X, Castaño E, Null D, Steichen J, Sánchez PJ, Ramilo O, et al. Safety and pharmacokinetics of an intramuscular humanized monoclonal antibody to respiratory syncytial virus in premature infants and infants with bronchopulmonary dysplasia. The MEDI-493 Study Group. Pediatr Infect Dis J. 1998; 17(9): p. 787–791. PMID: 9779762

21. Armitage RJ, Fanslow WC, Strockbine L, Sato TA, Clifford KN, Macduff BM A DM, et al. Molecular and biological characterization of a murine ligand for CD40. Nature. 1992; 357(6373): p. 80–82. https://doi.org/10.1038/357080a0 PMID: 1374165

22. Noelle RJ, Roy M, Shepherd DM, Stamenkovic I, Ledbetter JA, Aruffo A. A 39-kDa protein on activated helper T cells binds CD40 and transduces the signal for cognate activation of B cells. Proc. Natl. Acad. Sci. USA. 1992; 89(14): p. 6550–6554. PMID: 1378631

23. Karpusas M, Hsu YM, Wang JH, Thompson J, Lederman S, Chess L, et al. 2A crystal structure of an extracellular fragment of human CD40 ligand. Structure. 1995; 3(10): p. 1031–1039. PMID: 8589998

24. Pinchuk LM, Klaus SJ, Magaletti DM, Pinchuk GV, Norsen JP, Clark EA. Functional CD40 ligand expressed by human blood dendritic cells is up-regulated by CD40 ligation. J Immunol. 1996; 157(10): p. 4363–4370. PMID: 8906811

25. Grammer AC, Bergman MC, Miura Y, Fujita K, Davis LS, Lipsky PE. The CD40 ligand expressed by human B cells costimulates B cell responses. J Immunol. 1995; 154(10): p. 4996–5010. PMID: 7537298

26. Henn V, Slupsky JR, Gräfe M, Anagnostopoulos I, Förster R, Müller-Berghaus G, et al. CD40 ligand on activated platelets triggers an inflammatory reaction of endothelial cells. Nature. 1998; 391(6667): p. 591–594. https://doi.org/10.1038/35393 PMID: 9468137

27. Quezada SA, Jarvinen LZ, Lind EF, Noelle RJ. CD40/CD154 interactions at the interface of tolerance and immunity. Annu Rev Immunol. 2004; 22: p. 307–328. https://doi.org/10.1146/annurev.immunol.22.012703.104533 PMID: 15032580

28. Danese S S M F C. The CD40/CD40L costimulatory pathway in inflammatory bowel disease. Gut. 2004; 53(7): p. 1035–1043. https://doi.org/10.1136/gut.2003.026278 PMID: 15194658

29. van Mierlo GJ, den Boer AT, Medema JP, van der Voort EI, Fransen MF, Offringa R, et al. CD40 stimulation leads to effective therapy of CD40(-) tumors through induction of strong systemic cytotoxic T lymphocyte immunity. Proc Natl Acad Sci U S A. 2002; 99(8): p. 5561–5566. https://doi.org/10.1073/pnas.082107699 PMID: 11929985

30. Grossmann ME, Brown MP, Brenner MK. Antitumor responses induced by transgenic expression of CD40 ligand. Hum Gene Ther. 1997; 8(16): p. 1935–1943. https://doi.org/10.1089/hum.1997.8.16-1935 PMID: 9382959

31. Gravel C, Elmgren C, Muralidharan A, Hashem AM, Jaentschke B, Xu K, et al. Development and applications of universal H7 subtype-specific antibodies for the analysis of influenza H7N9 vaccines. Vaccine. 2015 Feb 25; 33(9):1129–34. 2015; 33(9): p. 1129–1134. https://doi.org/10.1016/j.vaccine.2015.01.034 PMID: 25620245

32. Hauser H, Shen L, Gu QL, Krueger S, Chen SY. Secretory heat-shock protein as a dendritic cell-targeting molecule: a new strategy to enhance the potency of genetic vaccines. Gene Ther. 2004; 11(11): p. 924–932. https://doi.org/10.1038/sj.gt.3302160 PMID: 15085173

33. Hashem AM, Gravel C, Chen Z, Yi Y, Tocchi M, Jaentschke B, et al. CD40 ligand preferentially modulates immune response and enhances protection against influenza virus. J Immunol. 2014; 193(2): p. 722–734. https://doi.org/10.4049/jimmunol.1300093 PMID: 24928989

34. Livak KJ, Schmittgen TD. Analysis of relative gene expression data using real-time quantitative PCR and the 2(-Delta Delta C(T)) Method. Methods. 2001; 25(4): p. 402–408. https://doi.org/10.1006/meth.2001.1262 PMID: 11846609

35. Reynolds CR, Islam SA, Sternberg MJE. EzMol: A web server wizard for the rapid visualisation and image production of protein and nucleic acid structures. J Mol Biol.

36. van Kooten C, Banchereau J. CD40-CD40 ligand. J Leuk Biol. 2000; 67: p. 2–17.

37. Aggarwal BB, Gupta SC, Kim J. Historical perspectives on tumor necrosis factor and its superfamily: 25 years later, a golden journey. Blood. 2012; 119(3): p. 651–665. https://doi.org/10.1182/blood-2011-04-325225 PMID: 22053109

38. Fiumara P, Younes A. CD40 ligand (CD154) and tumour necrosis factor-related apoptosis inducing ligand (Apo-2L) in haematological malignancies. British Journal of Haematology. 2001; 113: p. 265–274. PMID: 11380390

39. Song Y, Buchwald P. TNF Superfamily Protein–Protein Interactions: Feasibility of Small-Molecule Modulation. Current Drug Targets. 2015; 16(4): p. 393–408. PMID: 25706111

40. Peitsch MC, Jongeneel CV. A 3-D model for the CD40 ligand predicts that it is a compact trimer similar to the tumor necrosis factors. Int. Immunol. 1993; 5: p. 233–238. PMID: 8095800

41. Chan KH, Sonnenberg K, Niedrig M, Lam SY, Pang CM, Chan KM, et al. Use of Antibody Avidity Assays for Diagnosis of Severe Acute Respiratory Syndrome Coronavirus Infection. Clin Vaccine Immunol. 2007; 14(11): p. 1433–1436. https://doi.org/10.1128/CVI.00056-07 PMID: 17881505

42. Morris AE, Remmele RL Jr., Klinke R, Macduff BM, Fanslow WC, Armitage RJ. Incorporation of an isoleucine zipper motif enhances the biological activity of soluble CD40L (CD154). J. Biol. Chem. 1999; 274: p. 418–423. PMID: 9867859

43. Singh-Jasuja H, Thiolat A, Ribon M, Boissier MC, Bessis N, Rammensee HG, et al. The mouse dendritic cell marker CD11c is down-regulated upon cell activation through Toll-like receptor triggering. Immunobiol. 2013; 218(1): p. 28–39.

44. Masten BJ, Yates JL, Pollard Koga A M, Lipscomb MF. Characterization of accessory molecules in murine lung dendritic cell function: roles for CD80, CD86, CD54, and CD40L. Am J Respir Cell Mol Biol. 1997; 16: p. 335–342. https://doi.org/10.1165/ajrcmb.16.3.9070619 PMID: 9070619

45. Ma DY, Clark EA. The role of CD40 and CD40L in Dendritic Cells. Semin Immunol. 2009; 21(5): p. 265–272. https://doi.org/10.1016/j.smim.2009.05.010 PMID: 19524453

46. Mann J, Oakley F, Johnson PWM, Mann DA. CD40 Induces Interleukin-6 Gene Transcription in Dendritic Cells. J Biol Chem. 2002; 277(19): p. 17125–17138. https://doi.org/10.1074/jbc.M109250200 PMID: 11886848

47. Van Snick J. Interleukin-6: An Overview. Annu Rev Immunol. 1990; 8: p. 253–278. https://doi.org/10.1146/annurev.iy.08.040190.001345 PMID: 2188664

48. Akira S, Taga T, Kishimoto T. Interleukin-6 in Biology and Medicine. Adv. Immunol. 1993; 54: p. 1–78. PMID: 8379461

49. Banchereau J, Briere F, Caux C, Davoust J, Lebecque S, Liu YJ, et al. Immunobiology of Dendritic Cells. Annu. Rev. Immunol. 2000; 18: p. 767–811. https://doi.org/10.1146/annurev.immunol.18.1.767 PMID: 10837075

50. Grohmann U, Fallarino F, Bianchi R, Belladonna ML, Vacca C, Orabona C, et al. In vivo priming of T cells against cryptic determinants by dendritic cells exposed to interleukin 6 and native antigen. J Immunol. 2001; 167: p. 708–714.

51. Gurunathan S, Irvine KR, Wu CY, Cohen JI, Thomas E, Prussin C, et al. CD40 ligand/trimer DNA enhances both humoral and cellular immune responses and induces protective immunity to infectious and tumor challenge. J Immunol. 1998; 161: p. 4563–4571. PMID: 9794383

52. Noelle RJ, Mackey M, Foy T, Buhlmann J, Burns C. CD40 and its ligand in autoimmunity. Ann NY Acad Sci. 1997; 815: p. 384–391. PMID: 9186684